On the performances of a particle tracking detector based on triangular scintillator bars read out by silicon photomultipliers

On the performances of a particle tracking detector based on triangular scintillator bars read out by silicon photomultipliers

P. Bernardini[a,b], S. Cecchini[c], F. Cindolo[c], I. D'Antone[c], L. Degli Esposti[c], G. Fiore[b], I. Lax[c], G. Mandrioli[c], G. Marsella[a,b], N. Mauri[c,d], L. Pasqualini[c,d,*], L. Patrizii[c], C. Pinto[a,b], M. Pozzato[c], G. Sirri[c], A. Surdo[b], M. Tenti[c]

[a] *Dipartimento di Matematica e Fisica dell'Università del Salento, 73100 Lecce, Italy*
[b] *Istituto Nazionale di Fisica Nucleare, INFN, Sezione di Lecce, 73100 Lecce, Italy*
[c] *Istituto Nazionale di Fisica Nucleare, INFN, Sezione di Bologna, 40127 Bologna, Italy*
[d] *Dipartimento di Fisica e Astronomia, Università di Bologna, 40127 Bologna, Italy*

Abstract

A tracking detector composed of scintillator bars with a triangular cross-section read out by silicon photomultipliers in analog mode was developed. The tracker was designed to instrument a low density spectrometer for neutrino experiments. The performance of the system has been studied by exposing it to charged particle beams at the CERN-PS. The tests have shown that the position resolution in reconstructing charged particles' tracks is within 2.2 mm over the momentum range 0.5-10 GeV/c.

Keywords: Scintillators, SiPM, particle tracking device, position resolution.

1. Introduction

In 2011 a search for sterile neutrinos with a short baseline ν_μ beam experiment was proposed by the ICARUS-NESSiE Collaborations [1, 2]. The proposal foresaw two magnetized spectrometers (see Fig. 1 (a)) downstream of a LAr TPC at far and near sites along the neutrino beam, 1600 and 300 m away from the proton target, respectively. The spectrometers were designed to measure the charge sign and momentum of muons produced in ν_μ CC interactions. An iron core spectrometer would reconstruct muons up to $\sim$ 20 GeV/c [3], while an air core spectrometer put in front of the iron spectrometer would be dedicated to reconstruct low energy muons ($\sim$ 0.5-5 GeV/c). The proposed air spectrometer (see Fig. 1 (b)) was made of 39 Aluminum coils, 72×72 mm^2 cross-section with a circulating 2 A/mm^2 current density generating a magnetic field of 0.12 T in air volume 1.3 m deep. The air spectrometer would contain a tracking device (see Fig. 1 (b)) to separate μ^+/μ^- with the requirement of a charge misidentification below 3% at $\sim$ 1 GeV/c. For this purpose a Monte Carlo (MC) simulation showed that a tracking system with spatial resolution of O(mm) was required[1, 2].

This paper explores the performances of a tracking device made of scintillator bars read out by Silicon PhotoMultipliers (SiPM). Results obtained with a tracking detector prototype exposed to charged beams are reported.

2. Tracking detector design

The tracking detector is based on planes of extruded scintillator bars with triangular cross-section produced at FNAL [4]. The base of the triangle is (17.0 ± 0.5) mm and its height is (33.0 ± 0.5) mm as shown in Fig. 2. The bars, as sketched in Fig. 2, have a central hole with a diameter of (2.6 ± 0.2) mm where a WaveLength Shifter (WLS) fiber is glued. The lateral surface of the scintillator is coated with TiO_2. These bars had been already used in past neutrino experiments [5] with a readout based on photomultipliers tubes. The new design presented in this paper

*Corresponding Author: Dr. Laura Pasqualini, c/o INFN-Bologna, v.le Berti Pichat 6/2, 40127 Bologna, Italy;
Email: laura.pasqualini@bo.infn.it

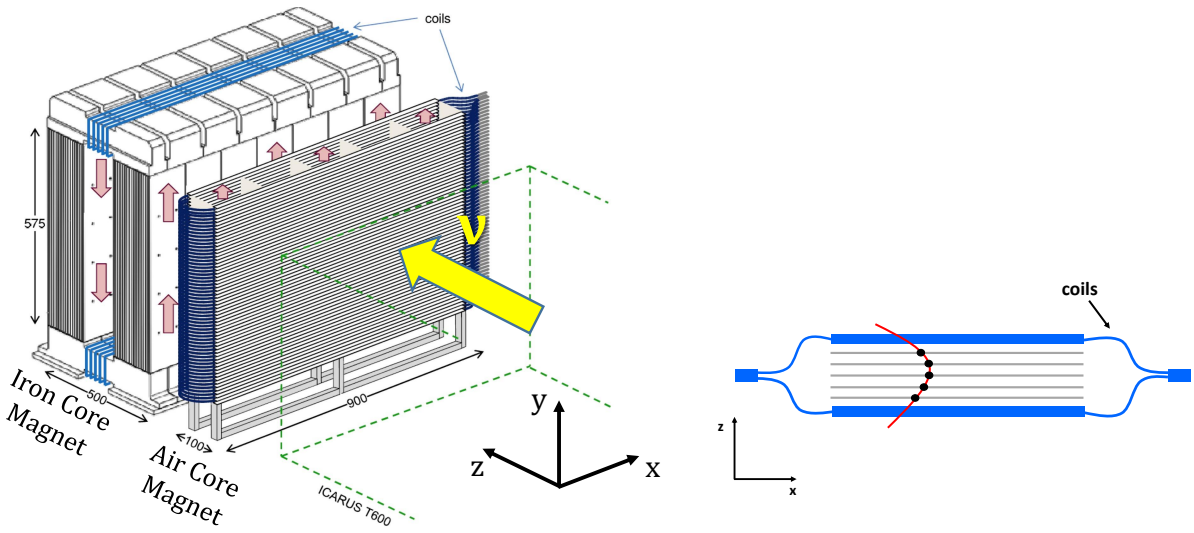

(a) (b)

Figure 1: (a) The two magnetic spectrometers: an Iron Core Magnet for the reconstruction of the momentum and charge of high energy muons placed downstream to an Air Core Magnet dedicated to the reconstruction of low momentum muons. (b) A top view of the Air Core Magnet: the magnet is made of Aluminum coils (blue lines), the internal detector planes (grey lines) are made of scintillator bars and the black dots represent the hit positions of a track.

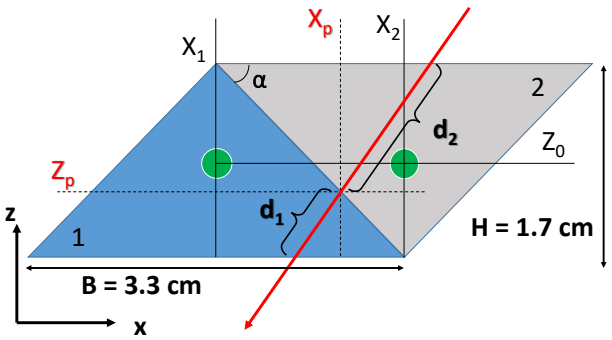

Figure 2: Couple of adjacent scintillator bars crossed by a charged particle (red arrow). X_1 and X_2 are the fiber positions of bars 1 and 2, d_1 and d_2 are the path length in each bar projected in the (x, z) plane, $\alpha = 45.88°$ is the angle at the base of the triangular bar, X_p and Z_p are the coordinates of the particle's impact point on the interface between the two scintillators and Z_0 is the nominal z coordinate of the plane.

foresees that bars are read out in analog mode by SiPMs. Features like single photon detection, reduced size, low power consumption and insensitivity to magnetic fields make these devices an optimal choice in designing a tracking detector operating in a magnetic field. Similar triangular bars have been used also for other applications, notably as muon tomography for studies in archeology, geology and civil engineering fields [6, 7] or for inspections of suspicious materials [8].

The transverse position X_p of a particle's impact point on the interface between two scintillators of a detector plane is reconstructed using the pulse height recorded by two adjacent detector channels. With reference to Fig. 2 the transverse position X_p is reconstructed as X_{rec}:

$$X_{rec} = \frac{(w_1 X_1 + w_2 X_2)}{(w_1 + w_2)} \tag{1}$$

where X_i $(i = 1, 2)$ is the fiber nominal transverse position and w_i is the pulse height of the i-th channel. At first order, assuming the response is linear, the signal height w_i is expected to be proportional to the particle energy release ΔE_i

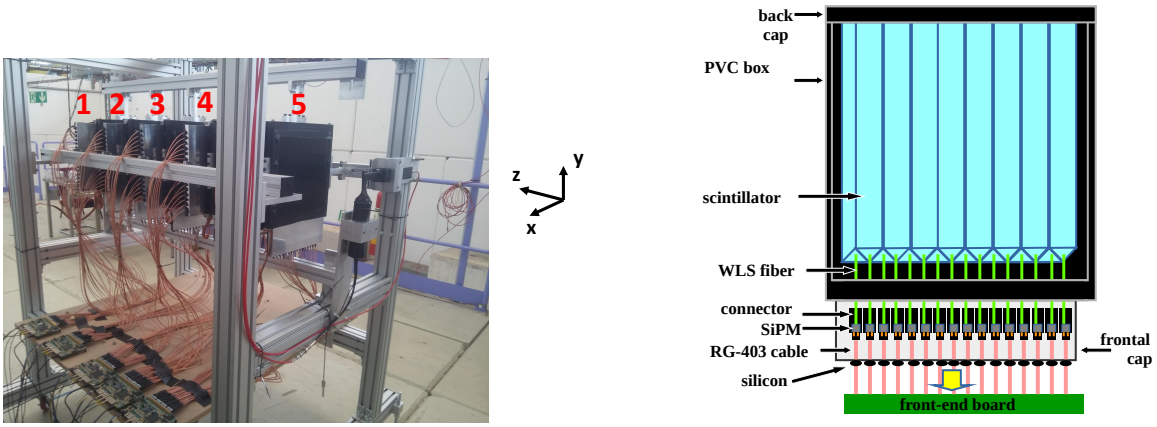

(a) (b)

Figure 3: (a) A picture of the tracking system mounted on its frame (numbers indicate the x and y tracking planes). The z-axis indicates the beam direction. (b) A sketch of a detector plane: it is composed of 16 scintillator bars inside a black PVC box. Fibers are coupled to SiPMs through a connector and the analog signal is sent to the front-end board by means of a triaxial RG-403 cable.

in each bar and therefore to the particle path length d_i ($w_i \propto \Delta E_i \propto d_i$). Hence Eq. (1) is a reasonable estimator of the particle position. A longitudinal reconstructed position (Z_{rec}) is associated to the reconstructed transverse position (X_{rec}):

$$Z_{rec} = Z_0 \pm \left[\frac{1}{2}(X_1 + X_2) - X_{rec}\right] \tan\alpha \tag{2}$$

where α is the angle at the base of the triangular bar and Z_0 is the fiber nominal longitudinal position. The sign + (-) is for couple of bars with the vertex angle of the first bar upstream (downstream) w.r.t. the particle direction. As a consequence, the longitudinal position associated to each reconstructed transverse position is not constant along the bar x direction.

A preliminary study of this tracking method, based on triangular scintillator bars, was performed with a table-top set-up exposed to cosmic rays [9]. It was shown that a spatial resolution better than 2 mm can be achieved.

3. Test of a tracking detector prototype

Based on the results reported in [9] a 5-module prototype of the tracker to instrument the air spectrometer (section 1) was designed and built for characterization with charged particle beams. The beam test allowed to select particles of known energy and direction and to collect large statistics. The modules were mounted on a rigid frame at fixed positions and spaced by 25 cm along the z direction (Fig. 3 (a)). The frame was mounted on wheels allowing to move and rotate it w.r.t the beam. Each module was composed of 2 orthogonal planes of 16 30 cm long scintillator bars. In Fig. 3 (b) a detector plane is shown in the (x, y) view. The scintillation light was collected by a 2 mm diameter WLS fiber (Kuraray Y11 [10] single cladding) coupled at one end to a SiPM SenSL microFC with an active area of 3×3 mm^2 [11]. The other end was mirrored using $\sim$ 0.1 mm thick Aluminum foil glued to the scintillator end cap. The SiPM was coupled to the fiber by a 3D printed custom connector. The overall number of electronic channels was 160 ($16 \times 2 \times 5$ planes).

The signals of SiPMs were read out by custom front end boards[1], one per module, each hosting a 32-channels EASIROC readout chip [12]. The first 16 channels were dedicated to read out the planes in the y direction, and the second set of 16 channels to read out the planes in the x direction. For each detector module the channel outputs were multiplexed on a common line thus providing a signal carrying the sequence of 32 SiPMs voltage values. The multiplexed outputs were acquired by a CAEN WaveForm Digitizer V1720 with a time sampling granularity of 250 MS/s and an ADC conversion with 12 bits.

[1]The front end board was developed by the Bologna INFN electronic group.

p (GeV/c)	negative beam (particles/spill)				positive beam (particles/spill)			
	e^-	π^-	$\overline{p}$	K^-	e^+	π^+	p	K^+
0.5	$2{\cdot}10^4$	$1{\cdot}10^4$	$<1{\cdot}10^2$	$1{\cdot}10^3$	$2{\cdot}10^4$	$1{\cdot}10^4$	$6{\cdot}10^3$	$1{\cdot}10^3$
5	$9{\cdot}10^3$	$1.7{\cdot}10^5$	$4{\cdot}10^2$	$1{\cdot}10^4$	$9{\cdot}10^3$	$2.7{\cdot}10^5$	$2{\cdot}10^5$	$3{\cdot}10^4$
10	$1{\cdot}10^3$	$8{\cdot}10^4$	50	$4{\cdot}10^3$	$1{\cdot}10^3$	$2{\cdot}10^5$	$7{\cdot}10^5$	$4{\cdot}10^4$

Table 1: Particles/spill of different beam components at different momenta and beam polarities.

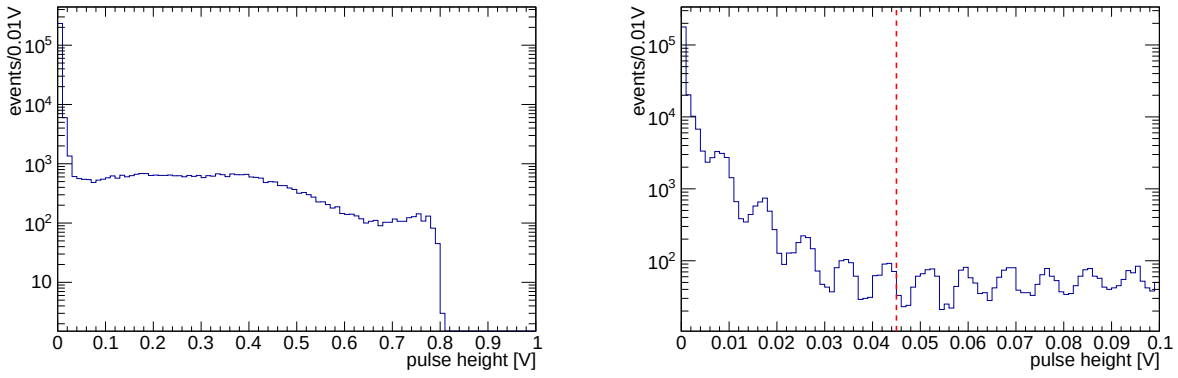

(a) (b)

Figure 4: (a) Pulse height distribution in one detector channel for a run of 5 GeV/c muons. (b) The same distribution up to 100 mV. The red dotted line indicates the trigger threshold at 45 mV.

3.1. Beam test

The tracking detector prototype was exposed to positive and negative particle beams in the 0.5-10 GeV/c momentum range at the CERN PS T9 beamline. The beam contained different fractions of pions, (anti)-protons, electrons or positrons and kaons as shown in Tab. 1 [13]. For some runs almost pure muons beams were obtained by means of a beam stopper. It is worth noting that the composition of the beam was not relevant in this study that was aimed at assessing the prototype tracking properties to minimum ionizing particles (m.i.p.s). A beam spill lasted for ~ 400 ms and the maximum particle rate per spill was ~ 10^6, achieved at 10 GeV/c for positive beam polarity, ensuring negligible pile-up probability. In the following each run, excepted muon runs, is identified by the beam polarity and momentum. During the data taking a delay wire chamber was used to monitor the beam (x, y) profile with a spatial resolution of 100-200 μm. The detector was placed at ~ 7 m from the beam pipe end. At this distance the beam was well contained and distributed over the detector. Overall, in about 320 runs with different beam energies, trigger selections and detector inclination, 3.6 millions of scintillator triggers (events) were recorded.

3.2. Data analysis

The signal amplitude for one photoelectron (p.e.) is ~ 8 mV determined from the multi-peak fit of the SiPM dark current pulse height distribution. A trigger on internal modules 2, 3 and 4 was normally used requiring at least one channel over a threshold of ~ 45 mV (i.e. ~ 5-6 p.e.) in each detector plane (x and y) of each modules. This trigger was a convenient choice to maximize data collection at any rotation of the detector. In few runs a trigger on 4 modules was used for efficiency measurements. The channel pulse heights were obtained by processing the digitizer waveforms with an offline analysis program. A baseline value was determined for each channel as the the mean of the Gaussian fit to its voltage distribution excluding p.e. signals. The channel pulse height w_i was computed by subtracting the baseline from its voltage value. In Fig. 4 (a) the pulse height distribution in a bar is shown for runs of 5 GeV/c muons. In Fig. 4 (b) the same distribution is shown for pulse heights < 100 mV: the dark current contribution dominates below 40 mV while above single peaks from beam particles are clearly visible. The shape of the pulse height distribution

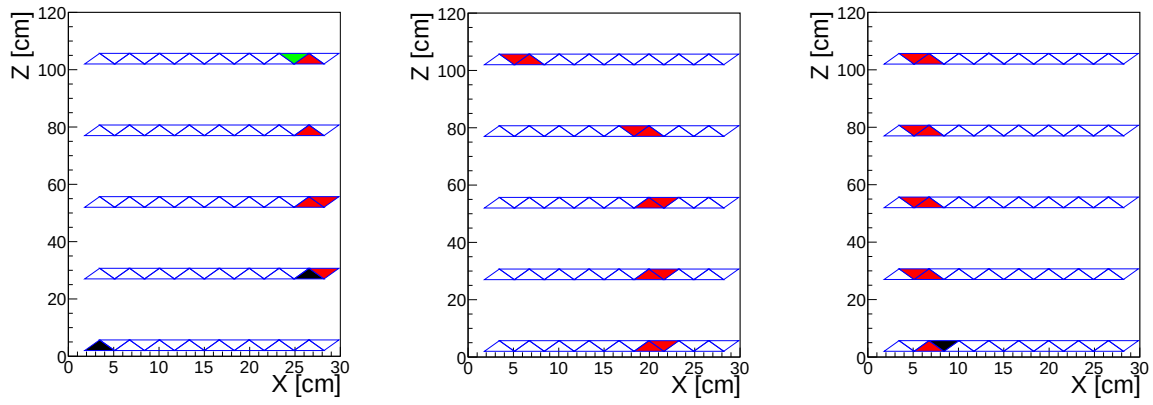

(a) (b) (c)

Figure 5: Display of three events from 5 GeV/c charged particles (the beam direction is from bottom to top). Black triangles indicate bars with signal amplitude < 20 mV, the green triangle indicates a bar with signal between 20 and 80 mV, and red triangles indicate bars with signals > 80 mV. In (a) and (b) are the displays of events removed from the data sample by requiring $\Delta^2 \leq 10$ cm^2 (see text); (c) event satisfying the condition $\Delta^2 \leq 10$ cm^2.

is almost flat because the beam particles crossing the bar have an uniform position distribution along the transverse direction.

Muon data were used to equalize detector channels. Their response can differ, for example, of bar to bar variation of optical couplings. For a given channel i of the $j-$th plane the median $m_{i,j}$ of its signal amplitude distribution was computed and the corresponding equalization factor $c_{i,j}$ was estimated as:

$$c_{i,j} = \frac{m_{i,j}}{\frac{1}{N}\sum_i^N m_{i,j}} \tag{3}$$

where N is the number of channels in each detector plane. The equalization factors differ by at most 20%.

The analysis procedure applied on test beam data is described below using a sample of 62000 events of a 5 GeV/c run in negative polarity. It should be noticed that no track finding algorithm was implemented but a simpler method, as explained in the following, was applied.

The first step of the analysis is the cluster identification. In order to reduce the dark current contribution, a cluster is defined as one bar or a collection of adjacent bars each with a signal > 10 mV. Events with only 1 cluster composed of 1 or 2 bars in each plane (x, y) were selected. This choice ensured the exclusion of showering particles reducing the event sample to 8% of the original one. The clusters' reconstructed x or y positions were determined using Eq. (1), after applying equalization factors to the signal amplitudes. The fiber nominal position was assigned to clusters with only one fired channel. A linear least-squares fit of the cluster's reconstructed positions was then performed for each selected event. An estimator was defined as the sum of squared residuals between the reconstructed positions $X_{rec,i}$ ($Y_{rec,i}$) and the fit positions $X_{fit,i}$ ($Y_{fit,i}$) over all planes at $Z_{fit,i} = Z_{rec,i}$:

$$\Delta^2 = \sum_i^5 (X_{rec,i} - X_{fit,i})^2 \tag{4}$$

By requiring $\Delta^2 \leq 10$ cm^2 events as those shown in Fig. 5 (a) and (b), due for example to scattering, decays or random dark current coincidences, were removed. In Fig. 5 (c) an event with $\Delta^2 \leq 10$ cm^2 is shown. Events with one fired channel at the edge of the detector plane were also discarded: for these channels the charge cannot be determined thus the uncertainty on the cluster position would be larger. The final sample, reduced to about 6% of the original one, included only events with straight particle tracks crossing all planes.

The distribution of the positions Y_{rec}, X_{rec} as reconstructed on the transverse plane (x, y) of the 1^{st} detector module is shown in Fig. 6 for 5 GeV/c particle tracks. The shape of the distribution reproduces what is expected from the

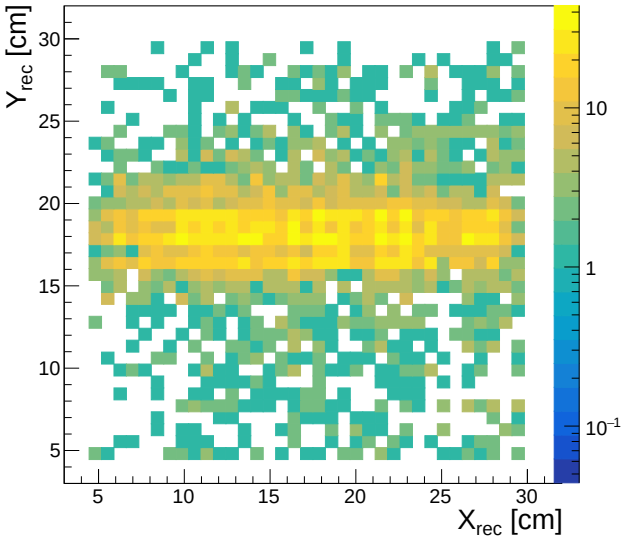

Figure 6: Reconstructed positions X_{rec}, Y_{rec} in the 1^{st} detector module for 5 GeV/c particle tracks.

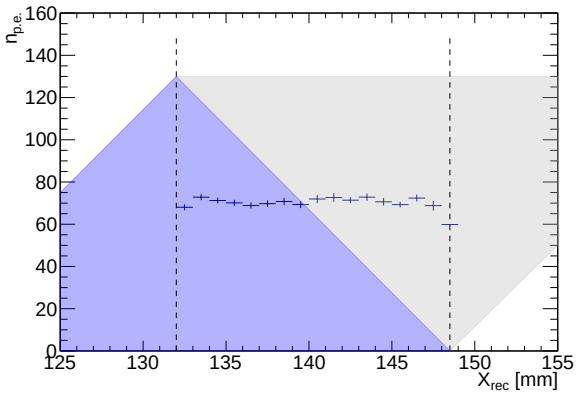

Figure 7: Mean of the sum of the number of collected p.e. ($n_{p.e.}$) in a couple of adjacent channels with signals > 10 mV as a function of the reconstructed position in the plane obtained selecting tracks with a slope < 50 mrad in the (x, z) view.

beam: ~ 25 cm wide along the x direction with a mean track slope of $< \theta_x >= -4.6$ mrad, and ~ 5 cm wide along the y direction with $< \theta_y >= 0.3$ mrad.

Systematic errors due to the mechanical misalignments along the transverse x and y directions of detector planes were corrected by fitting linearly the reconstructed positions of tracks with only 1 cluster of 1 or 2 bars in each plane, and estimating the position offsets of each detector plane. Systematic errors due to slight rotations of detector planes, were estimated < 0.6 mrad from the mechanical design.

In Fig. 7 the mean of the sum of collected p.e. in a couple of adjacent bars with signals > 10 mV is shown as a function of the reconstructed position for tracks with a slope < 50 mrad in the longitudinal (x, z) view; ~ 70 p.e. were collected for m.i.p. particles almost perpendicular to the plane.

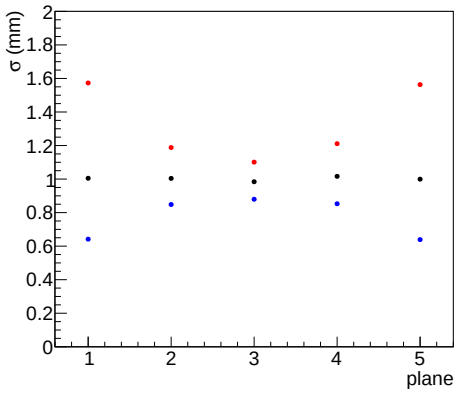

Figure 8: Position resolutions σ_{in} (blue), σ_{ex} (red) and geometric mean σ (black) of each plane obtained with a toy MC.

4. Results

4.1. Detector position resolution

In the following data are compared with a realistic optical MC simulation of the detector, based on Geant4. The optical MC takes into account the emission and absorption spectra of the scintillator and of the fiber, parametrized as a function of the photon wavelength, as well as the attenuation length of the scintillator [4], of the fiber core and of the fiber cladding [10]. The reflectivity of the TiO_2 painting and the SiPM Photon Detection Efficiency (PDE) were simulated as a function of the photon wavelength as reported in the datasheets [11, 14]. The simulation does not include the dark current and the front end electronics dynamic range. Moreover, for each beam energy only the most abundant particle component was simulated (ref. Tab. 1).

The position resolution in a given plane was determined as follows: a linear fit to the reconstructed positions in all planes was performed in the (x, z), (y, z) views. The residuals in the chosen plane between the reconstructed positions, X_{rec}, and the fit positions, X_{fit}, were computed. The width of the Gaussian fit to the distribution of residuals was defined as σ_{in}. Similarly, σ_{ex} was defined as the width of the Gaussian fit to the distribution of residuals obtained by excluding the same plane from the linear fit. Given the limited number of detector planes, a correct estimate of the position resolution is provided by the geometric mean [15]:

$$\sigma = \sqrt{\sigma_{in} \cdot \sigma_{ex}} \tag{5}$$

A toy MC was used to verify that the geometric mean is a good estimator of the position resolution. Tracks were generated with random slopes uniformly distributed; the track positions were calculated in each plane at five evenly spaced longitudinal z coordinates. The reconstructed positions X_{rec} along the x direction in each plane were calculated applying a Gaussian smearing (σ_{true} = 1 mm) to the track position. The position resolutions σ_{in} (blue) and σ_{ex} (red) are shown for each plane in Fig. 8. In the figure black dots represent the spatial resolution σ obtained with Eq. (5), which reproduces the expected resolution σ_{true}.

The distribution of residuals evaluated excluding the 3^{rd} x plane from the fit is shown in Fig. 9 (a) for data (red) and events generated with the optical MC (blue). Gaussian fits to the data and MC distributions yield the widths $\sigma_{ex-data}$ = (1.68 ± 0.02) mm and σ_{ex-MC} = (1.56 ± 0.02) mm, respectively. A linear fit of the reconstructed positions using all planes was performed; the corresponding distribution of the residual in the 3^{rd} x plane is shown in Fig. 9 (b) for data and MC. The width of the Gaussian fit to the distribution is $\sigma_{in-data}$ = (1.34 ± 0.02) mm for the data and σ_{in-MC} = (1.26 ± 0.01) mm for the MC.

The position resolutions for 5 GeV/c negative particles are shown in Fig. 10 for each (x, z) (a), (y, z) (b) plane and they are compared with the optical MC. The statistical errors are negligible. For data the mean values for the (x, z) and (y, z) planes are $\sigma_X \sim 1.49$ mm and $\sigma_Y \sim 1.36$ mm, respectively, to be compared with the mean values obtained with MC: $\sigma_X \sim 1.43$ mm and $\sigma_Y \sim 1.37$ mm. The (y, z) planes have a better position resolution than (x, z) planes. As discussed in the following the position resolution worsens as the track slope increases. As shown in Fig. 6, the beam

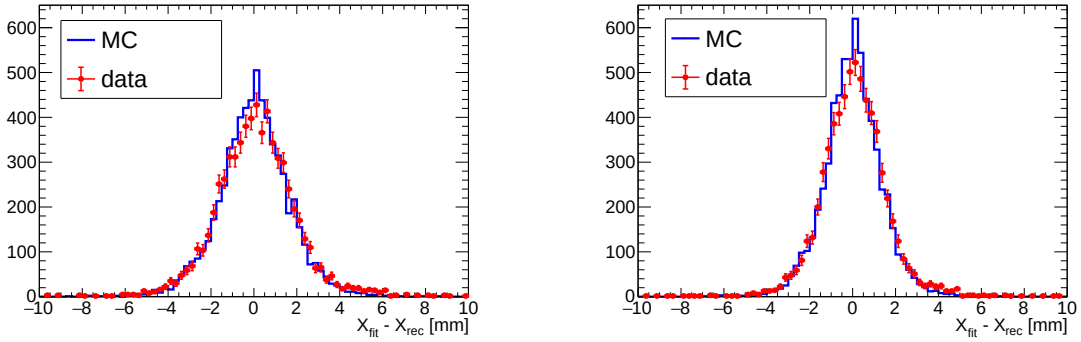

(a) (b)

Figure 9: (a) The distribution of residuals $X_{fit} - X_{rec}$ on a plane not included in the fit for data (red dots) and MC (blue histogram). The widths of the distributions are $\sigma_{ex-data}$ = (1.68 ± 0.02) mm and σ_{ex-MC} = (1.56 ± 0.02) mm for data and MC, respectively. (b)The distribution of residuals $X_{fit} - X_{rec}$ on a plane included in the fit: the widths of the distributions are $\sigma_{in-data}$ = (1.34 ± 0.02) mm for the data and σ_{in-MC} = (1.26 ± 0.01) mm for the MC. The errors on σ are the statistical errors.

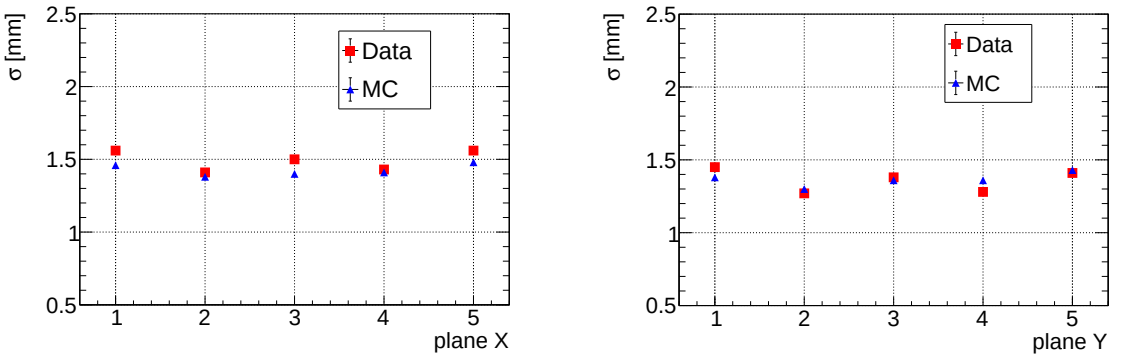

(a) (b)

Figure 10: (a) Position resolutions of the (x, z) planes and (b) of the the (y, z) planes for data (red) and MC (blue) obtained as geometric mean between σ_{ex} and σ_{in}.

is narrower in the y direction and wider in the x direction. Similar results for the position resolutions were obtained with positive beam polarity data.

In order to evaluate the dependence of the position resolution on the track slope data with the detector tilted at different angles with respect to the beam axis (-5° and -10°) were collected. Figure 11 (a) shows the average position resolution for (x, z) planes versus the track slope (θ_X) for 5 GeV/c particle for data and MC events. A slight worsening of about 0.2 mm in the position resolution is observed at larger angles both for experimental and simulated data.

The average position resolution of x and y planes as a function of the particle momentum is shown in Fig. 11 (b) for runs in negative beam polarity. At 0.5 GeV/c the beam was mainly composed of electrons, while at 5 GeV/c and 10 GeV/c pions were the most abundant particles. The Multiple Coulomb Scattering (MCS) leads to a worsening of the position resolution at lower momenta. The contribution of MCS, larger at lower energies [16], enlarges the particle displacement along the x and y directions, thus increasing the width of the distributions of residuals in each plane.

Based on the results obtained with 30 cm long bars, the use of bars several meter long was investigated by means of the optical MC simulation. Muons of 5 GeV/c were simulated impinging vertically on couples of adjacent scintillator bars up to 3 m long. The residuals between the true particle impact points and the positions reconstructed with Eq. (1) were computed. A position resolution of ∼ 2 mm was obtained for 3 m bars.

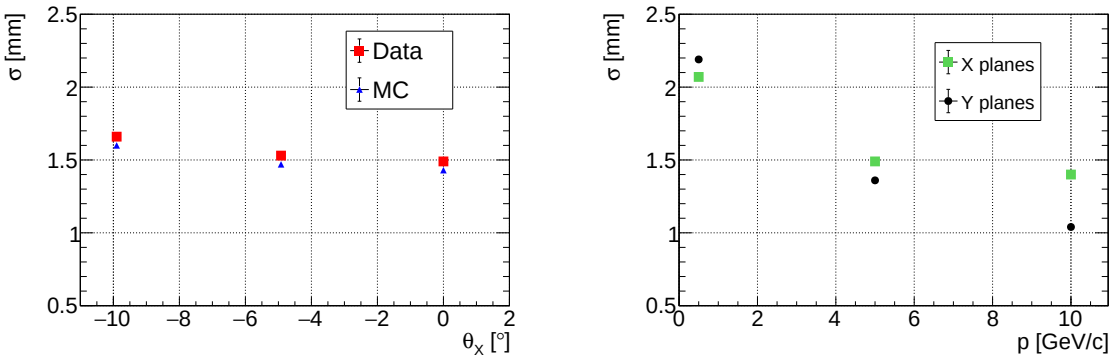

(a) (b)

Figure 11: (a) Average position resolutions for (x, z) planes versus the track slope θ_X for data (red) and MC (blue). (b) Average position resolutions of all x (green) and y (black) planes for runs in negative beam polarity and at different particle momentum: 0.5, 5 and 10 GeV/c.

4.2. Detector efficiency

In order to evaluate the plane efficiency different runs were performed excluding from the trigger one module at a time. Events with only 1 cluster of 1 or 2 bars in the planes included in the trigger were selected and reconstructed positions were fitted by a straight line. Events in which the projection of the fit position on the plane excluded from the trigger is within the detector geometrical acceptance were selected and counted as N_s. The number (N) of events with 1 cluster in the excluded plane having a residual ≤ 5 times the position resolution were counted. The efficiency of the plane was evaluated as N/N_s. Efficiencies $> 98\%$ were found for all detector planes.

4.3. Dependence of the residuals on the transverse reconstructed position

The residuals versus the transverse reconstructed position for the 1^{st} x plane are shown in Fig. 12 (a). The x interval shown in the figure refers to the region between two adjacent bar fibers. Muon data are compared with 5 GeV/c simulated muons impinging perpendicularly to the bars. The residuals are larger towards the corner of the triangular bars and are minimum at the center of the region. In Fig. 12 (a) the x interval is divided in three regions and the corresponding distributions of residuals are plotted in Fig. 12 (b). Average values are positive/negative for regions closer to the corner of the bars (left/right histograms); in the central region the residual distribution is centered on $X_{fit} - X_{rec} = 0$.

Deviations from linearity of the collected light in a bar w.r.t. the energy deposited were investigated with the optical MC simulation. The ratio between the energy deposited and the number of p.e. collected in one bar is shown for simulated events in Fig. 13 versus the transverse reconstructed position in the plane. The ratio between the energy deposited and collected photons is almost constant along the transverse direction X_{rec} increasing at the corner of the bar. As a consequence the X_{rec} is biased towards the corner position thus widening the distribution of residuals.

4.4. Charge mis-identification

The capability of the tracking detector to separate μ^+ and μ^- was estimated with the optical MC simulation of the apparatus. Negative muons with momentum ranging from 0.5 to 5 GeV/c were generated crossing the tracker placed in an air volume with a magnetic field of 0.12 T. A parabolic fit, $x = az^2 + bz + c$, to the reconstructed positions was performed. The charge sign was reconstructed if $|a| > 3\,\sigma_a$, where σ_a is the statistical error on the a parameter. The charge mis-identification, evaluated as the ratio of the number of events with a wrong charge sign to the number of events with a reconstructed charge, is shown in Fig. 14 as a function of the μ^- momentum. A charge mis-ID $< 3\%$ is obtained for $p_\mu \leq 2$ GeV/c.

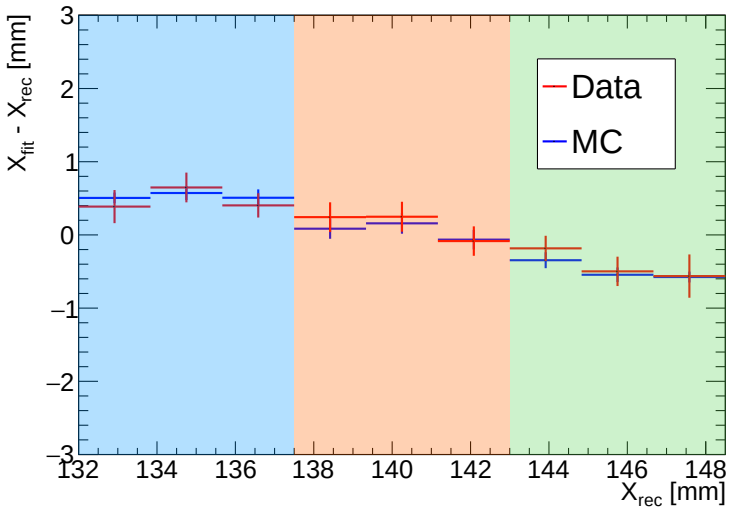

(a)

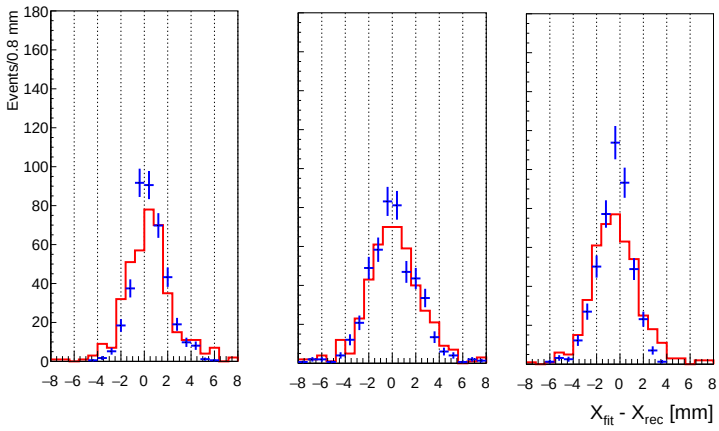

(b)

Figure 12: (a) Residuals versus reconstructed position for the 1^{st} x plane for data (red) and MC (blue). For each bin the mean values of residuals and the corresponding errors are displayed. To highlight the dependence of the residuals on the position along the bar, the area between the two adjacent bars is divided in three regions depicted with three different colours: light blue for $132 < X_{rec} \leq 137.5$ mm, orange for $137.5 < X_{rec} \leq 143$ mm and green for $143 < X_{rec} \leq 148.5$ mm. (b) residual distributions for $132 < X_{rec} \leq 137.5$ mm (left histogram), $137.5 < X_{rec} \leq 143$ mm (central histogram) and $143 < X_{rec} \leq 148.5$ mm (right histogram).

5. Conclusions and perspectives

A tracking device was developed to achieve a position resolution in the few mm range for the reconstruction of O(1 GeV) muon tracks using a system made of planes of cm size triangular scintillator bars. A tracking detector prototype was tested with charged beams at CERN PS. Results show that the position resolution ranges from 2.2 to 1.4 mm over the 0.5-10 GeV/c interval. Furthermore, the plane efficiency is larger than 98% for all planes. The charge mis-identification, estimated with simulated events, is $< 3\%$ for $p_\mu \leq 2$ GeV/c. The performances of this system, i.e. its efficiency and position resolution, together with its scalability and moderate cost make it attractive for the detection of muons in large neutrino oscillation experiments, for example as a component of the near detector beam monitoring system.

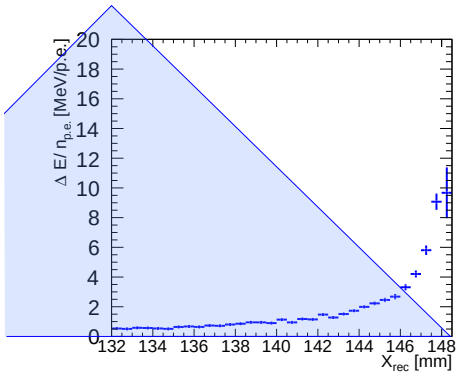

Figure 13: Histogram profile of the ratio between the energy deposited and the number of p.e. collected in one bar as a function of the reconstructed position in the plane for MC events. The blue triangle represents the bar profile.

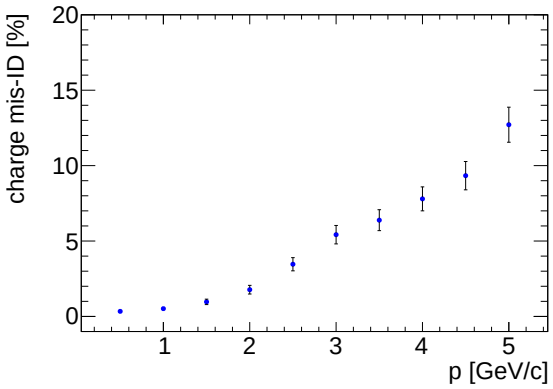

Figure 14: Charge mis-identification as a function of the particle momentum. The vertical bars indicate the statistical errors.

6. Acknowledgements

This project has received funding from the European Union's Horizon 2020 Research and Innovation programme under the Grant Agreement no. 654168. The authors gratefully acknowledge CERN and the PS staff for successfully operating the East Experimental Area and for continuous supports to the users. Finally, the authors gratefully thank the workshops of INFN Bologna and Lecce for the construction of the tracking prototype.

References

[1] P. Bernardini, et al., NESSiE Collaboration, SPSC-P-343 (2011).
[2] M. Antonello, et al., ICARUS-NESSiE Collaboration, SPSC-P-347 (2012).
[3] A. Anokhina, et al., Eur. Phys. J. C (2017) 77: 23.
[4] A. Pla-Dalmau, et al., Nucl. Instrum. Methods A 466 (2001) 482.
[5] L. Aliaga, et al., MINERvA Collaboration, Nucl. Instrum. Methods A 743 (2014) 130.
[6] A. Anastasio, et al., MU-RAY Collaboration, Nucl. Instrum. Methods A 718 (2013) 134.
[7] G. Baccani, et al., J. Instrum. 13 (2018) no.11, P11001.
[8] V. Anghel, et al., Nucl. Instrum. Methods A 798 (2015) 12.
[9] S. Cecchini, et al., Nucl. Instrum. Methods A 846 (2017) 1.
[10] http://kuraraypsf.jp/psf/ws.html
[11] http://sensl.com/downloads/ds/DS-MicroCseries.pdf
[12] S. Callier, et al., Phys. Procedia 37 (2012) 1569.
[13] http://gatignon.web.cern.ch/gatignon/T9flux.pdf
[14] https://www.chemours.com/TitaniumTechnologies/esUS/techinfo/literature/Coatings/COBH65969CoatingsBrochure.pdf

[15] R. K. Carnegie, et al., Nucl. Instrum. Methods A 538 (2005) 372.
[16] J. Beringer et al., (Particle Data Group) Phys. Rev. D 86 (2012) 010001.